

Evidence for charged critical fluctuations in underdoped $\text{YBa}_2\text{Cu}_3\text{O}_{7-\delta}$

T. Schneider¹, R. Khasanov^{1,2,3}, K. Conder², E. Pomjakushina², R. Bruetsch⁴ and H. Keller¹

⁽¹⁾ *Physik-Institut der Universität Zürich, Winterthurerstrasse 190, CH-8057, Switzerland*

⁽²⁾ *Laboratory for Neutron Scattering, ETH Zürich and PSI Villigen, CH-5232 Villigen PSI, Switzerland*

⁽³⁾ *DPMC, Université de Genève, 24 Quai Ernest-Ansermet, 1211 Genève 4, Switzerland*

⁽⁴⁾ *Laboratory for Material Behavior, PSI Villigen, CH-5232 Villigen PSI, Switzerland*

We report and analyze in-plane penetration depth measurements in $\text{YBa}_2\text{Cu}_3\text{O}_{7-\delta}$ taken close to the critical temperature T_c . In underdoped $\text{YBa}_2\text{Cu}_3\text{O}_{6.59}$ we find consistent evidence for charged critical behavior. Noting that the effective dimensionless charge $\tilde{e} = \xi/\lambda = 1/\kappa$ scales as $T_c^{-1/2}$, this new critical behavior should be generically observable in suitably underdoped cuprates.

Close to the critical temperature T_c of the normal-superconductor transition, in a regime roughly given by the Ginzburg criterion [1–4], order parameter fluctuations dominate critical properties. In recent years, the effect of the charge of the superconducting order parameter in this regime in three dimensions has been studied extensively [5–15]. While for strong type-I materials, the coupling of the order parameter to transverse gauge field fluctuations is expected to render the transition first order [6], it is well-established that strong type-II materials should exhibit a continuous phase transition, and that sufficiently close to T_c , the charge of the order parameter is relevant [8–15]. However, in cuprate superconductors within the fluctuation dominated regime, the region close to T_c , where the system crosses over to the regime of charged fluctuations turns out to be too narrow to access. For instance, optimally doped $\text{YBa}_2\text{Cu}_3\text{O}_{7-\delta}$, while possessing an extended regime of critical fluctuations, is too strongly type-II to observe charged critical fluctuations [1–4,16]. Indeed, the effective dimensionless charge $\tilde{e} = \xi/\lambda = 1/\kappa$ is in strongly type II superconductors ($\kappa \gg 1$) small. The crossover upon approaching T_c is thus initially to the critical regime of a weakly charged superfluid where the fluctuations of the order parameter are essentially those of an uncharged superfluid or XY-model [1]. Furthermore, there is the inhomogeneity induced finite size effect which renders the asymptotic critical regime unattainable [17,18]. However, underdoped cuprates could open a window onto this new regime because κ is expected to become rather small. Here the cuprates undergo a quantum superconductor to insulator transition in the underdoped limit [4,19–22] and correspond to a 2D disordered bosonic system with long-range coulomb interactions. Close to this quantum transition T_c , λ_{ab} and ξ_{ab} scale as $T_c \propto \lambda_{ab}^{-2} \propto \xi^{-z}$ [4,19–22], yielding with the dynamic critical exponent $z = 1$ [4,22–25], $\kappa_{ab} \propto \sqrt{T_c}$. Noting that T_c decreases by approaching the underdoped limit, sufficiently homogeneous and underdoped cuprates appear to be potential candidates to observe charged critical behavior.

Here we report and analyze in-plane penetration depth measurements of underdoped $\text{YBa}_2\text{Cu}_3\text{O}_{7-\delta}$ to explore the evidence for this new critical behavior. $\text{YBa}_2\text{Cu}_3\text{O}_{7-\delta}$ samples were synthesized by solid-state reactions using high-purity Y_2O_3 , BaCO_3 and CuO . The samples were calcinated at 880–935°C in air for 100 h with several intermediate grindings. The phase-purity of the material was examined by powder x-ray diffraction. As synthesized, the samples have oxygen contents in the range 6.975–6.985. Starting with a material of maximal oxygen content a series of reduced samples have been produced. Our characterization revealed that the equilibration of the samples in closed ampoules with an appropriate amount of copper powder reacting with oxygen leads to the best results. Thus, for each sample in the series, an alumina crucible with Y123 powder of exactly known weight and oxygen content was placed in a quartz ampoule together with an exactly weighted copper powder in an another crucible. To ensure a homogenous oxygen distribution the ampoule was sealed under vacuum and heated up to 700°C (heating rate 10°C/h), kept at this temperature for 10h and finally slowly cooled (5°C/h). Field-cooled (FC) magnetization measurements were performed with a Quantum Design SQUID magnetometer in a field of 0.5 mT for temperatures ranging from 5 K to 100 K. The Meissner fraction f was the deduced from the mass of the samples and the x-ray density, and assuming spherical grains. To calculate the temperature dependence of the effective penetration depth $\lambda_{eff}(T)$ we used the Shoenberg formula [26,27] assuming spherical grains of radius R , particle size distribution $N(R)$ and volume fraction distribution $g(R) = N(R)R^3$,

$$f(T) = \int_0^\infty \left(1 - \frac{3\lambda(T)}{R} \cot\left(\frac{R}{\lambda(T)}\right) + \frac{3\lambda^3(T)}{R^2} \right) / \int_0^\infty g(R) dR \quad (1)$$

We extracted the grain size distribution $N(R)$ from an analysis of SEM (scanning electron microscope) photographs. Solving this nonlinear equation for given $f(T)$ and $g(R)$ we obtained the effective penetration depth $\lambda_{eff}(T)$. For sufficiently anisotropic superconductors ($\lambda_c/\lambda_{ab} > 5$), including $\text{YBa}_2\text{Cu}_3\text{O}_{7-\delta}$, λ_{eff} is proportional to the in-plane penetration depth, so that $\lambda_{eff} = 1.31\lambda_{ab}$ [28]. The resulting data for $\lambda_{ab}(T)$ agrees well with the transverse-field μSR measurements performed on similar samples [29].

When charged fluctuations dominate the in-plane penetration depth and the correlation length are related by [10–12,14,15]

$$\lambda_{ab} = \kappa_{ab}\xi_{ab}, \quad \lambda_{ab} = \lambda_{0ab}|t|^{-\nu}, \quad \nu \simeq 2/3, \quad (2)$$

contrary to the uncharged case, where $\lambda \propto \sqrt{\xi}$ and with that

$$\lambda_{ab} = \lambda_{0ab}|t|^{-\nu/2}, \quad (3)$$

where $t = T/T_c - 1$. In a plot $(d \ln \lambda_{ab}/dT)^{-1}$ versus T charged critical behavior is then uncovered in terms of a temperature range where the data falls on a line with slope $1/\nu \simeq 3/2$, while in the neutral (3D-XY) case it collapses on a line with slope $2/\nu \simeq 3$. Clearly, in an inhomogeneous system the phase transition is rounded and $(d \ln \lambda_{ab}/dT)^{-1}$ does not vanish at T_c . In Fig. 1 we displayed $(d \ln \lambda_{ab}/dT)^{-1}$ versus T for $\text{YBa}_2\text{Cu}_3\text{O}_{6.59}$, derived from the measured in-plane penetration depth data. The data uncover a crossover from uncharged critical behavior (dashed line) to charged criticality (solid line) with $T_c \simeq 56.1$ K, limited by a finite size effect due to the finite extent of the grains and/or inhomogeneities within the grains. Although charged criticality is attained there is no sharp transition. Indeed, λ_{ab} does not diverge at T_c because the correlation length $\xi_{ab} = \lambda_{ab}/\kappa_{ab}$ cannot grow beyond the limiting length L_{ab} in the ab -plane.

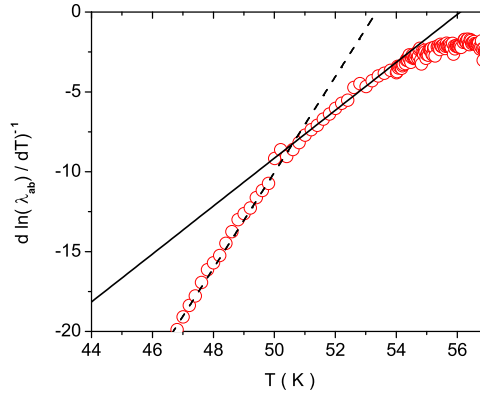


FIG. 1. $(d \ln \lambda_{ab}/dT)^{-1}$ with λ_{ab} in μm versus T for $\text{YBa}_2\text{Cu}_3\text{O}_{6.59}$. The straight line with slope $1/\nu \simeq 3/2$ corresponds according to Eq. (2) to charged criticality with $T_c = 56.1$ K, while the dashed line indicates the intermediate 3D-XY critical behavior with slope $2/\nu \simeq 3$.

To explore the evidence for charged critical behavior and the nature of the finite size effect further, we displayed in Fig. 2 $1/\lambda_{ab}$ and $d(1/\lambda_{ab})/dT$ vs. T . The solid line is $\lambda_{ab} = \lambda_{0ab}|t|^{-\nu}$ with $\lambda_{0ab} = 0.089 \mu\text{m}$, $\nu = 2/3$ and $T_c = 56.1$ K, appropriate for charged criticality, and the dashed one its derivative. Approaching T_c of the fictitious homogeneous system the data reveals again a crossover from uncharged to charged critical behavior, while the tail in λ_{ab} vs. T above $d\lambda_{ab}/dT$ points to a finite size effect. Indeed, $d\lambda_{ab}/dT$ does not diverge at $d\lambda_{ab}/dT$ but exhibits an extremum at $T_p \simeq 54.27$ K, giving rise to an inflection point in $\lambda_{ab}(T)$ at T_p . Here the correlation length attains the limiting length.

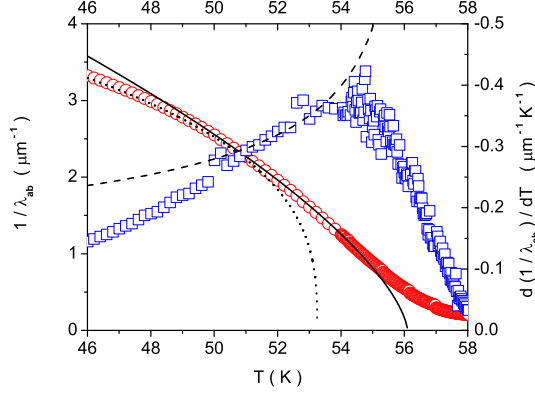


FIG. 2. $1/\lambda_{ab}$ and $d(1/\lambda_{ab})/dT$ vs. T for $\text{YBa}_2\text{Cu}_3\text{O}_{6.59}$. The solid line is $\lambda_{ab} = \lambda_{0ab} |t|^{-\nu}$ with $\lambda_{0ab} = 0.089 \mu\text{m}$, $\nu = 2/3$ and $T_c = 56.1$ K, appropriate for charged criticality, and the dashed one its derivative. The dotted line indicates uncharged critical behavior.

In this case the penetration depth adopts the finite size scaling form [30,31]

$$\lambda_{ab}(T) = \lambda_{0ab} |t|^{-\nu} g(y), \quad y = \text{sign}(t) \left| \frac{t}{t_p} \right|, \quad (4)$$

where $\xi_{ab}(T_p) = \xi_{0ab} |t_p|^{-\nu} = L_{ab}$. For t small and $L_{ab} \rightarrow \infty$ the scaling variable tends to $y \rightarrow \pm\infty$ where $g(y \rightarrow -\infty) = 1$ and $g(y \rightarrow +\infty) = 0$ while for $t = 0$ and $L_{ab} \neq 0$, $g(y \rightarrow 0) = g_0 |y|^\nu = g_0 |t/t_p|^\nu$. In this limit we obtain

$$\frac{\lambda_{ab}(T_c, L_{ab})}{\lambda_{0ab}} = g_0 \frac{L_{ab}}{\xi_{0ab}}. \quad (5)$$

Another essential property of the finite size scaling function stems from the existence of an inflection point in $\lambda_{ab}(T)$. It implies an extremum in $d\lambda_{ab}/dT$ at $T_p > T_c$ and with that the scaling form $g^+(y) = y^\nu (1 + f(y))$ with $df/dy \neq 0$ and $d^2f/dy^2 = 0$ at $y = 1$, e.g. $f(y) = ay + b(1-y)^3 + c$. In Fig. 3 we displayed the finite size scaling function $g(y)$ deduced from the measured data with $\lambda_{0ab} = 0.089 \mu\text{m}$, $\nu = 2/3$, $T_c = 56.1$ K and $T_p \simeq 54.27$ K. The solid line indicates the asymptotic behavior $g(y \rightarrow 0) = g_0 |y|^\nu$ with $g_0 = 0.42$. The upper branch corresponding to $T < T_c$ tends to $g(y \rightarrow -\infty) = 1$, while the lower one referring to $T > T_c$ approaches $g(y \rightarrow +\infty) = 0$. Consequently, the absence of a sharp transition (see Figs. 1 and 2), is fully consistent with a finite size effect arising from a limiting length L_{ab} in the ab -plane, attributable to the finite extent of the grains and/or inhomogeneities within the grains.

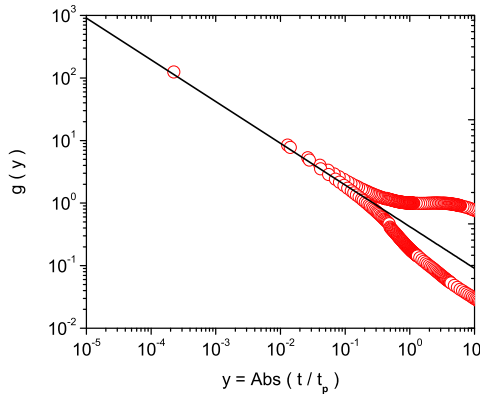


FIG. 3. Finite size scaling function $g(y)$ deduced from the measured data with $\lambda_{0ab} = 0.089 \mu\text{m}$, $\nu = 2/3$, $T_c = 56.1$ K and $T_p \simeq 54.27$ K. The solid line indicates the asymptotic behavior $g(y \rightarrow 0) = g_0 |y|^\nu$ with $g_0 = 0.42$.

To disentangle these options we note that $L_{ab}/\xi_{0ab} \simeq 51$ follows from the finite size scaling analysis by invoking Eq. (5) with $\lambda_{ab}(T_c, L_{ab}) \simeq 1.898 \mu\text{m}$, $\lambda_{ab0}(T_c, L_{ab}) \simeq 0.089 \mu\text{m}$ and $g_0 = 0.42$. Noting that $\xi_{ab0} = \gamma\xi_{c0}$, where γ is the anisotropy, we obtain with $\gamma \approx 20$ [32] and $\xi_{c0} \approx 10 \text{ \AA}$, appropriate for $\text{YBa}_2\text{Cu}_3\text{O}_{6.59}$ [33], the estimate $L_{ab} \approx 510 \text{ \AA}$ compared to $L_{ab} \approx 572 \text{ \AA}$ found in $\text{YBa}_2\text{Cu}_3\text{O}_{6.7}$ [18]. On the other hand, a glance to Fig.4 shows that the grain size distribution of our $\text{YBa}_2\text{Cu}_3\text{O}_{6.59}$ sample exhibits a maximum at $2R = 2800 \text{ \AA}$ and decreases steeply for smaller grains. Hence, the smeared transition is not attributable to the finite extent of the grains but due to inhomogeneities within the grains. However, this does not point at bad sample quality but at a genuine feature of underdoped cuprates reflecting the large value of ξ_{ab0} in this doping regime.

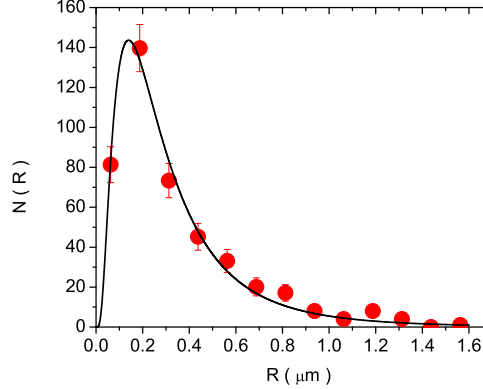


FIG. 4. Grain size distribution $N(R)$ of our $\text{YBa}_2\text{Cu}_3\text{O}_{6.59}$ sample derived from an analysis of SEM (scanning electron microscope) photographs. The solid line is a fit to the log-normal distribution [34].

Nevertheless, our analysis of the in-plane penetration depth data of underdoped $\text{YBa}_2\text{Cu}_3\text{O}_{6.59}$ provides remarkable consistency for critical fluctuations, consistent with the charged universality class, limited close to T_c of the fictitious infinite and homogeneous counterpart by a inhomogeneity induced finite size effect. Since $\kappa_{ab} \propto \sqrt{T_c}$ this will no longer hold true in the optimally doped counterparts. In this doping regime there is mounting evidence for neutral (3D-XY) critical behavior [3,4,16,22,33]. A prominent example is $\text{YBa}_2\text{Cu}_3\text{O}_{6.95}$ revealing in the in-plane penetration depth [16] 3D-XY behavior over three decades in reduced temperature, with no sign pointing to a crossover to charged criticality.

In summary, we have presented in-plane penetration depth data for $\text{YBa}_2\text{Cu}_3\text{O}_{6.59}$ providing consistent evidence for the charged critical behavior of the superconductor to normal state transition in type II superconductors ($\kappa > 1/\sqrt{2}$). Since the effective dimensionless charge $\tilde{e} = \xi/\lambda = 1/\kappa$ scales as $T_c^{-1/2}$ this new critical behavior should be observable and generic in suitably underdoped cuprates. In this regime the crossover upon approaching T_c is thus to the charged critical regime, while near optimum doping it is to the critical regime of a weakly charged superfluid where the fluctuations of the order parameter are essentially those of an uncharged superfluid (3D-XY). Furthermore, there is the inhomogeneity induced finite size effect which renders the asymptotic critical regime and with that the charged regime of nearly optimally doped samples difficult to attain.

ACKNOWLEDGMENTS

The authors are grateful to D. Di Castro, I. F. Herbut, S. Kohout, K.A. Müller, J. Roos, A. Shengelaya and Z. Tesanovic for very useful comments and suggestions on the subject matter. This work was partially supported by the Swiss National Science Foundation and the NCCR program *Materials with Novel Electronic Properties* (MaNEP) sponsored by the Swiss National Science Foundation.

[1] D. S. Fisher, M. P. A. Fisher and D. A. Huse, Phys. Rev. B **43**, 130 (1991).

- [2] T. Schneider and D. Ariosa, Z. Phys. B **89**, 267 (1992).
- [3] T. Schneider and H. Keller, Int. J. Mod. Phys. B **8**, 487 (1993).
- [4] T. Schneider and J. M. Singer, *Phase Transition Approach To High Temperature Superconductivity*, (Imperial College Press, London, 2000).
- [5] S. Coleman and E. Weinberg, Phys. Rev. D **7**, 1988 (1973).
- [6] B. I. Halperin, T. C. Lubensky, and S. K. Ma, Phys. Rev. Lett. **32**, 292 (1974).
- [7] C. Dasgupta and B. I. Halperin, Phys. Rev. Lett. **47**, 1556 (1981).
- [8] S. Kolnberger and R. Folk, Phys. Rev. B **41**, 4083 (1990).
- [9] M. Kiometzis, H. Kleinert, and A. M. J. Schakel, Phys. Rev. Lett. **73**, 1975 (1994); Fortschr. Phys. **43**, 697 (1995).
- [10] I. F. Herbut and Z. Tesanovic, Phys. Rev. Lett. **76**, 4588 (1996).
- [11] I. F. Herbut, J. Phys. A **30**, 423 (1997).
- [12] P. Olsson and S. Teitel, Phys. Rev. Lett., **80**, 1964 (1998).
- [13] R. Folk and Y. Holovatch, in *Correlations, Coherence, and Order*, edited by D.V. Shopov and D.I. Uzunov (Kluwer Academic Plenum, New York, 1999), pp. 83116.
- [14] J. Hove and A. Sudbø, Phys. Rev. Lett., **84**, 3426 (2000).
- [15] S. Mo, J. Hove, A. Sudbø, Phys. Rev. B **65**, 104501 (2002).
- [16] S. Kamal, D. A. Bonn, N. Goldenfeld, P. J. Hirschfeld, R. Liang, and W. N. Hardy, Phys. Rev. Lett. **73**, 1845 (1994); S. Kamal, R. Liang, A. Hosseini, D. A. Bonn, and W. N. Hardy, Phys. Rev. B **58**, R8933 (1998).
- [17] T. Schneider, Journal of Superconductivity, **17**, 41 (2004).
- [18] T. Schneider and D. Di Castro, Phys. Rev. B **69**, 024502 (2004).
- [19] T. Schneider and J. M. Singer, J. of Superconductivity **13**, 789 (2000).
- [20] T. Schneider and H. Keller, Phys. Rev. Lett. **86**, 4899 (2001).
- [21] T. Schneider, Physica B **326**, 289 (2003).
- [22] T. Schneider, cond-mat/0204236.
- [23] M.P.A. Fisher, G. Grinstein, and S. M. Girvin, Phys. Rev. Lett. **64**, 587 (1990).
- [24] Min-Chul Cha, M. P. A. Fisher, M. Wallin, and A. P. Young, Phys. Rev. B **44**, 6883 (1991).
- [25] I. F. Herbut, Phys. Rev. B **6**, 14723 (2000).
- [26] D. Shoenberg, Proc. R. Soc. Lond. **A 175**, 49 (1940).
- [27] A. Porch *et al.*, Physica C **214**, 350 (1993).
- [28] V. I. Fesenko, V. N. Gorbunov and V. P. Smilga, Physica C **176**, 551 (1991).
- [29] P. Zimmerman, H. Keller, S.L. Lee, I.M. Savic, M. Warden, D. Zech, R. Cubitt, E.M. Forgan, E. Kaldis, J. Karpinski, and C. Krüger, Phys. Rev. B **52**, 541 (1995).
- [30] J. L. Cardy ed., *Finite-Size Scaling*, North Holland, Amsterdam 1988.
- [31] N. Schultka and E. Manousakis, Phys. Rev. B **52**, 7528 (1995).
- [32] B. Janossy, D. Prost, S. Pekker and L. Fruchter, Physics C **181**, 51 (1991).
- [33] T. Schneider, cond-mat/0406340.
- [34] J. Kiefer and J.B. Wagner, J. Electrochem. Soc. **135**, 198 (1988).